

Supporting information

Chiral and kryptoracemic Dy(III) complexes with field-induced single molecule magnet behavior

Ying-Ying Zhang^a, Jing-Tao Yu^a, Bo Li^{b,*} De-Jing Li^c, Zhi-Gang Gu^c, Xiao-Fan Sun^d,

Hong-Ling Cai^d, George E. Kostakis^e Guo Peng^{a,*}

^aHerbert Gleiter Institute of Nanoscience, School of Materials Science and
Engineering, Nanjing University of Science and Technology, 210094 Nanjing, P. R.
China

Email: guopeng@njust.edu.cn

^bCollege of Chemistry and Pharmaceutical Engineering, Nanyang Normal University,
Nanyang 473061, P. R. China
Email: libozzu0107@163.com

^cState Key Laboratory of Structural Chemistry, Fujian Institute of Research on the Structure of Matter, Chinese Academy of Sciences, 350002 Fuzhou, P. R. China

^dCollaborative Innovation Center of Advanced Microstructures, Lab of Solid State Microstructures, School of Physics, Nanjing University, Nanjing 210093, P. R. China.

^eDepartment of Chemistry, School of Life Sciences, University of Sussex, Brighton,
BN1 9QJ, UK

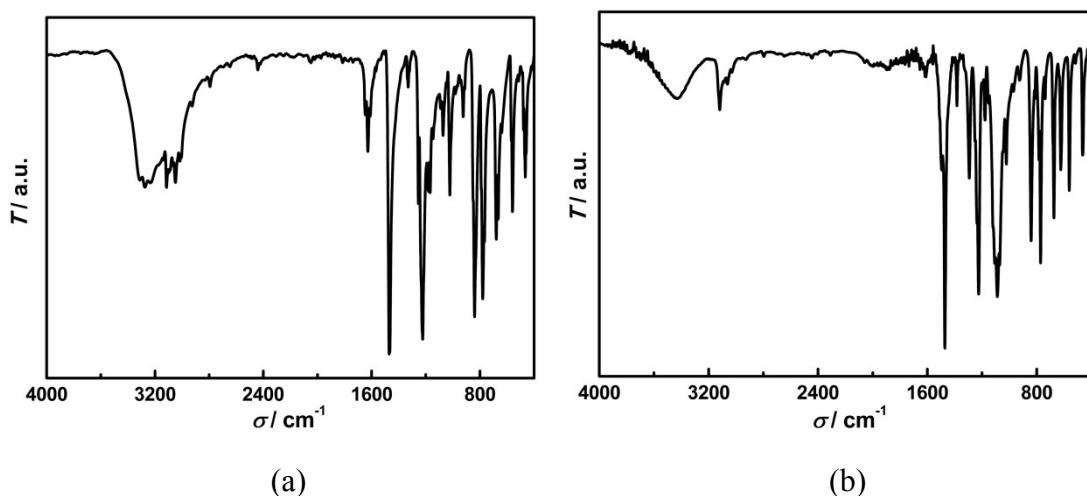


Fig. S1 IR spectra for complexes **1** (a) and **2** (b).

Table S1 Various experiments were carried out for crystalline products.

Lanthanide salts	The ratio of PNO to Dy ions	Solvent	Products
DyBr ₃ ·6H ₂ O	7:1	CH ₃ CN	1
Dy(ClO ₄) ₃ ·6H ₂ O	7:1 / 10:1 / 12:1 / 16:1	CH ₃ CN / CH ₃ OH / C ₂ H ₅ OH / CH ₃ CN+ C ₂ H ₅ OH	×
Dy(NO ₃) ₃ ·6H ₂ O	7:1	CH ₃ CN+C ₂ H ₅ OH / CH ₃ CN+CH ₃ OH	×
Dy(OAc) ₃ ·4H ₂ O	7:1	CH ₃ CN / CH ₃ CN+C ₂ H ₅ OH / CH ₃ CN+CH ₃ OH	×
Dy(OTf) ₃	7:1 / 8:1 / 10:1	CH ₃ CN / C ₂ H ₅ OH / CH ₃ OH	×
Dy(NO ₃) ₃ ·6H ₂ O+DyCl ₃ ·6H ₂ O	7:1 (14:1:1)	CH ₃ CN	×
Dy(NO ₃) ₃ ·6H ₂ O+Dy(ClO ₄) ₃ ·6H ₂ O	7:1 (35:2:3 / 21:1:2)	C ₂ H ₅ OH	2
Dy(NO ₃) ₃ ·6H ₂ O+ Dy(OTf) ₃	7:1 (35:1:4)	C ₂ H ₅ OH	×
Dy(OTf) ₃ +Dy(acac) ₃	7:1 (35:4:1)	C ₂ H ₅ OH	×

Table S2 Continuous shape measures (CShM) for complexes **1** and **2**.

Complexes	Ions	SAPR (D_{4d})	TDD (D_{2d})	JBTPR (C_{2v})	BTPR (C_{2v})
1	Dy1	1.928	0.488	2.328	1.534
2	Dy1	1.271	2.001	2.672	1.981
	Dy2	1.689	2.429	2.323	1.687

SAPR = Square antiprism, TDD = Triangular dodecahedron, JBTPR = Biaugmented trigonal prism J50, BTPR = Biaugmented trigonal prism.

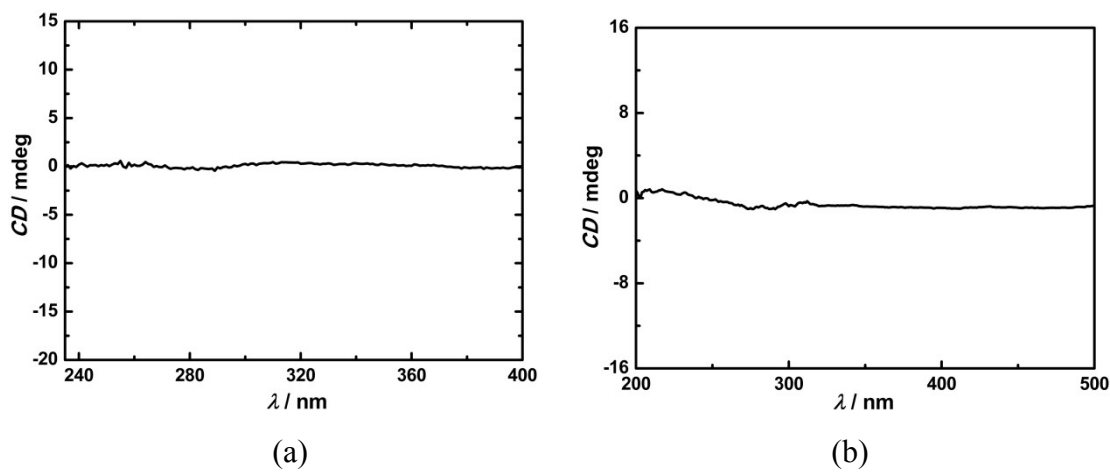
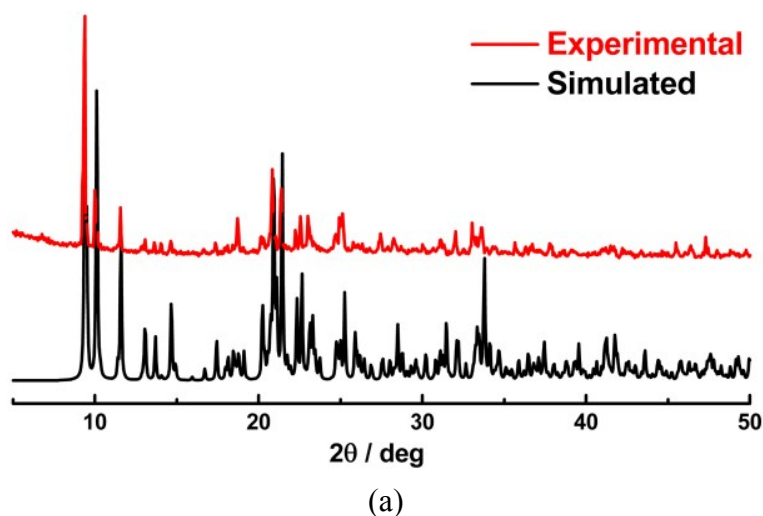


Fig. S2 Solid-state CD spectra of bulk samples for complexes **1** (a) and **2** (b).



(a)

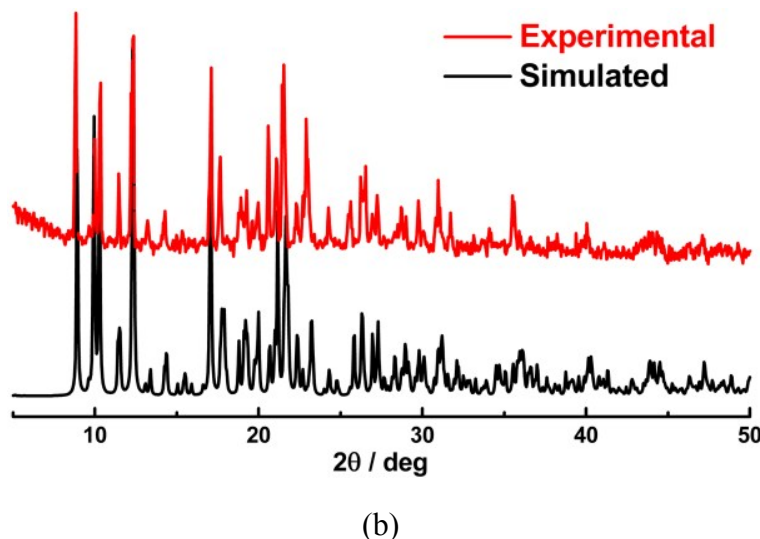


Fig. S3 Experimental and simulated PXRD patterns for complexes **1** (a) and **2** (b).

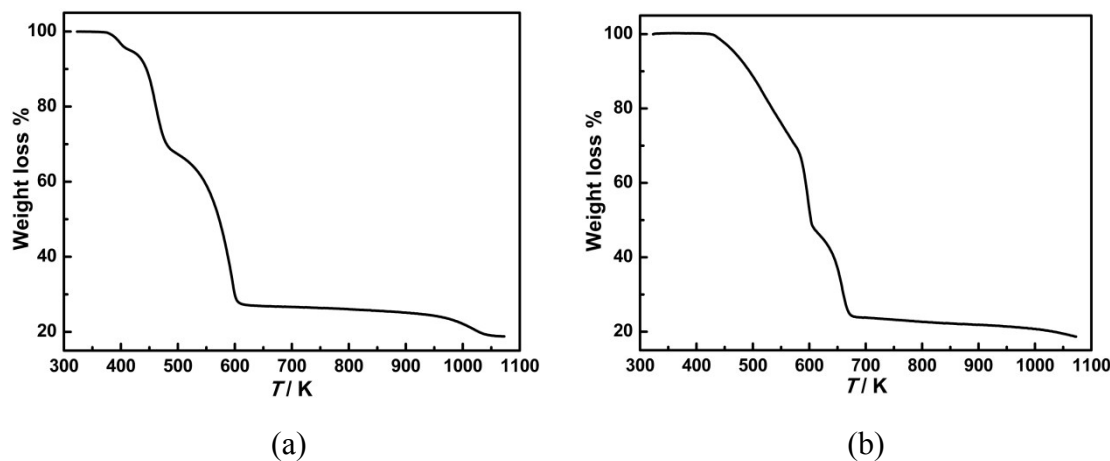


Fig. S4 TGA curves for complexes **1** (a) and **2** (b).

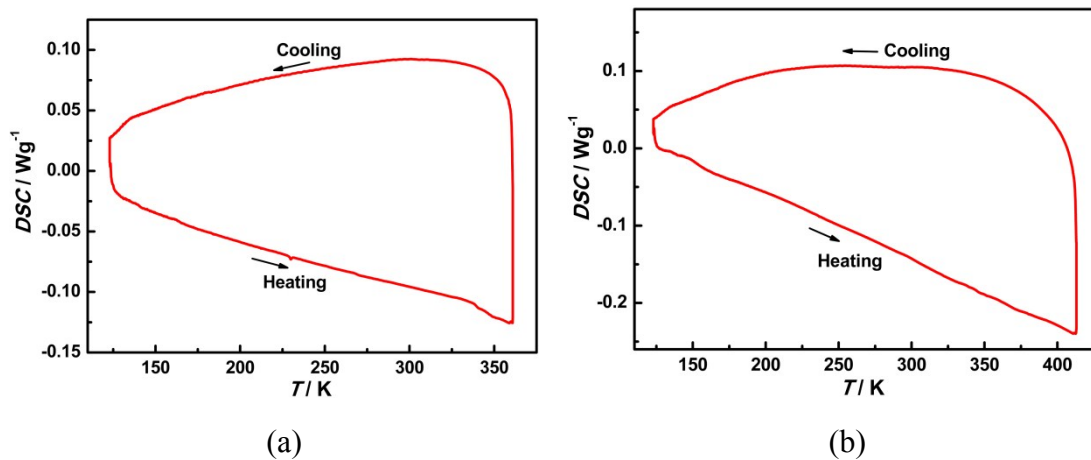


Fig. S5 DSC curves for complexes **1** (a) and **2** (b).

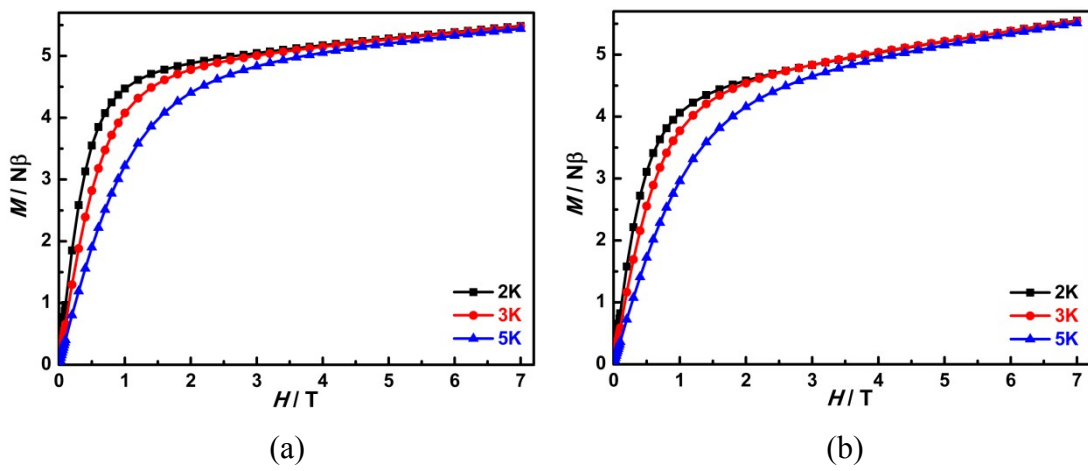


Fig. S6 M vs. H plots for complexes **1** (a) and **2** (b).

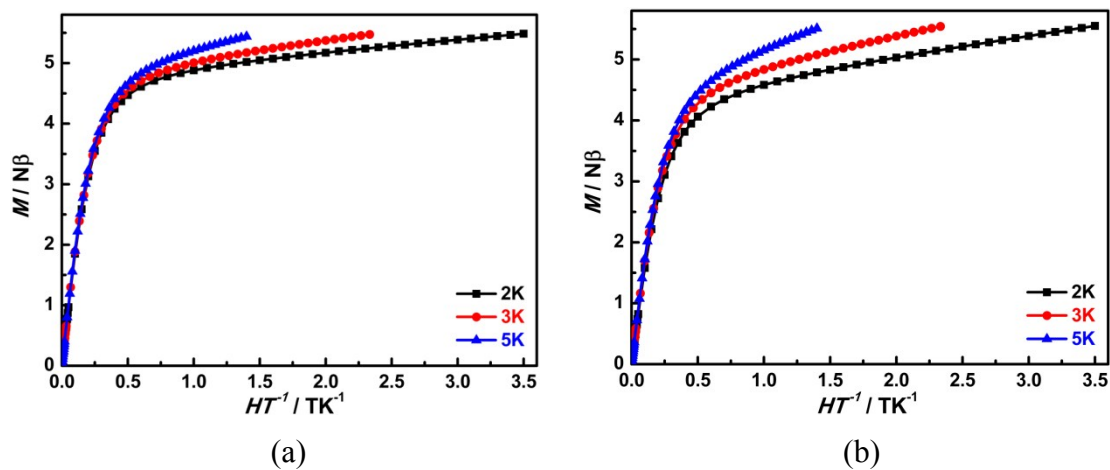


Fig. S7 M vs. HT^{-1} plots for complexes **1** (a) and **2** (b).

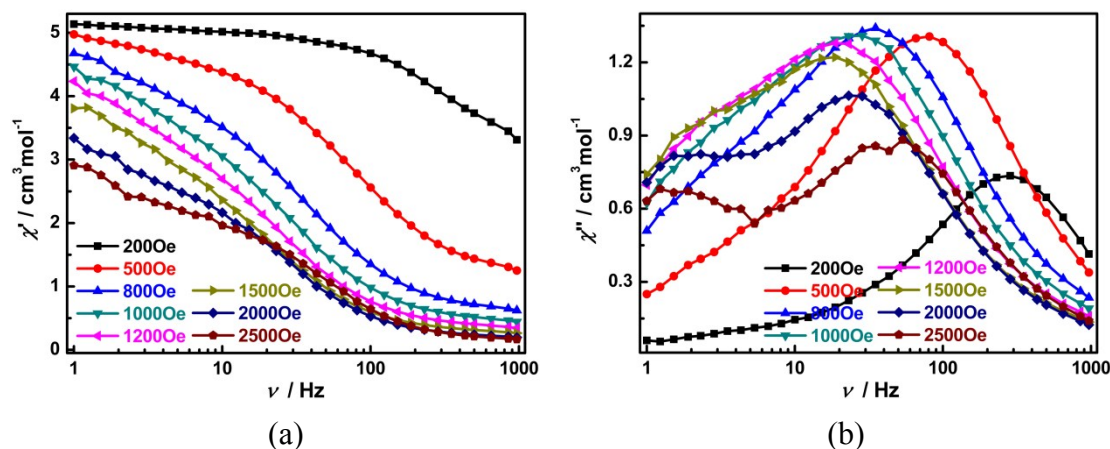


Fig. S8 Frequency dependence of in-phase (a) and out-of-phase (b) ac susceptibility signals under different dc fields at 2K for **1**.

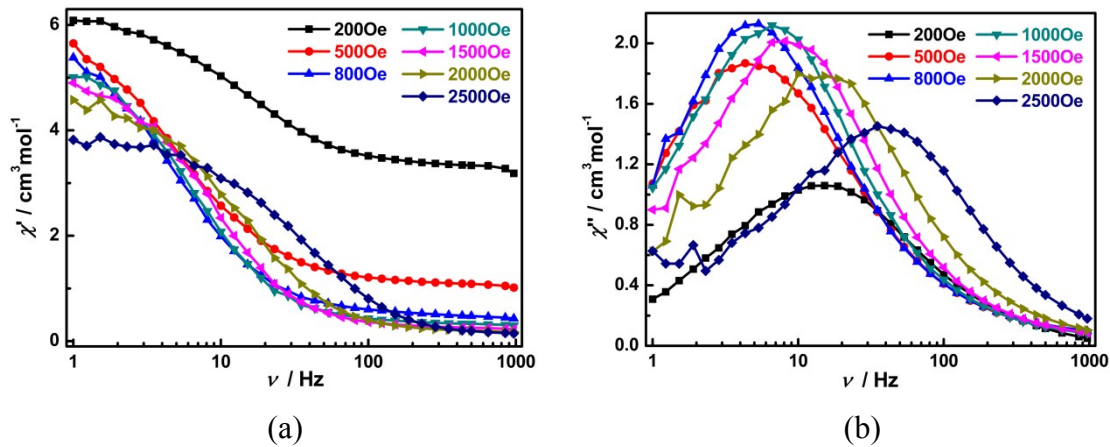


Fig. S9 Frequency dependence of in-phase (a) and out-of-phase (b) ac susceptibility signals under different dc fields at 2K for **2**.

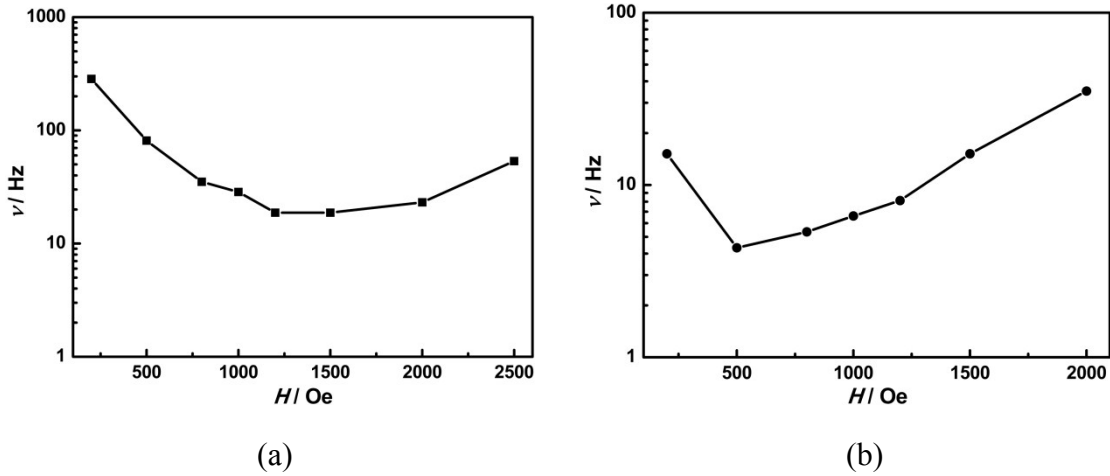


Fig. S10 Field dependence of the characteristic frequency for complexes **1** (a) and **2** (b) at 2K.

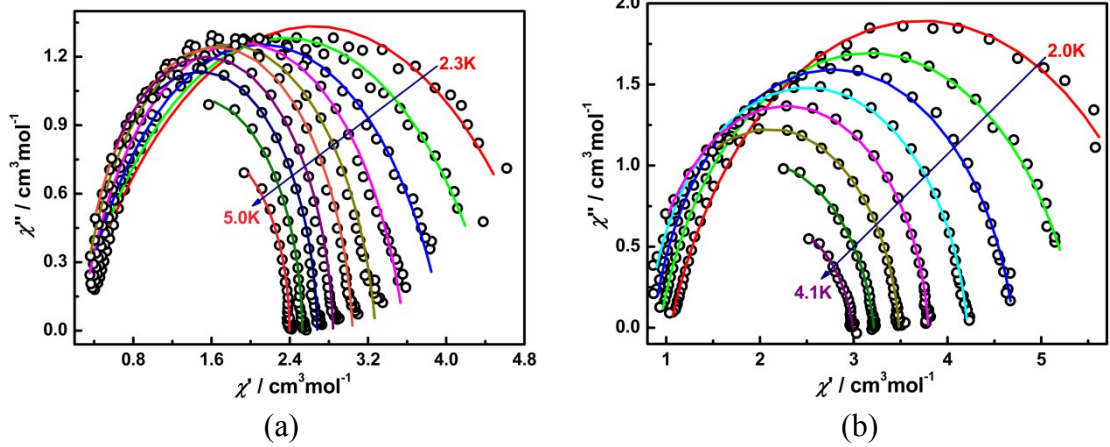


Fig. S11 The Cole-Cole plots for complexes **1** (a) and **2** (b). The solid lines are the

best fits to a generalized Debye model.

Table S3 Cole-Cole parameters of **1** under 1200Oe dc field.

T / K	$\chi_s / \text{cm}^{-3}\text{mol}^{-1}$	$\chi_T / \text{cm}^{-3}\text{mol}^{-1}$	τ / s	α	R
2.3	1.93E-01	5.10E+00	1.38E-02	3.66E-01	2.60E-01
2.6	2.11E-01	4.52E+00	9.01E-03	3.16E-01	1.71E-01
2.9	2.37E-01	3.98E+00	5.52E-03	2.47E-01	1.00E-01
3.2	2.63E-01	3.57E+00	3.20E-03	1.70E-01	7.22E-02
3.5	2.57E-01	3.28E+00	1.74E-03	1.17E-01	8.07E-02
3.8	2.55E-01	3.04E+00	8.91E-04	7.22E-02	4.87E-02
4.1	2.49E-01	2.84E+00	4.57E-04	4.94E-02	4.10E-02
4.4	2.92E-01	2.68E+00	2.42E-04	3.19E-02	2.73E-02
4.7	4.37E-01	2.53E+00	1.38E-04	2.00E-02	1.72E-02
5.0	8.16E-01	2.40E+00	9.48E-05	7.86E-03	1.10E-02

Table S4 Cole-Cole parameters of **2** under 500Oe dc field.

T / K	$\chi_s / \text{cm}^{-3}\text{mol}^{-1}$	$\chi_T / \text{cm}^{-3}\text{mol}^{-1}$	τ / s	α	R
2	1.04E+00	6.41E+00	3.42E-02	2.17E-01	4.90E-02
2.3	9.28E-01	5.39E+00	1.24E-02	1.73E-01	1.90E-02
2.6	8.61E-01	4.71E+00	4.57E-03	1.19E-01	3.22E-02
2.9	8.02E-01	4.21E+00	1.75E-03	8.87E-02	2.08E-02
3.2	7.67E-01	3.80E+00	6.84E-04	6.40E-02	2.32E-02
3.5	7.16E-01	3.48E+00	2.73E-04	7.58E-02	1.77E-02
3.8	7.71E-01	3.21E+00	1.16E-04	1.15E-01	1.05E-02
4.1	1.40E+00	2.99E+00	8.09E-05	1.49E-01	1.09E-02

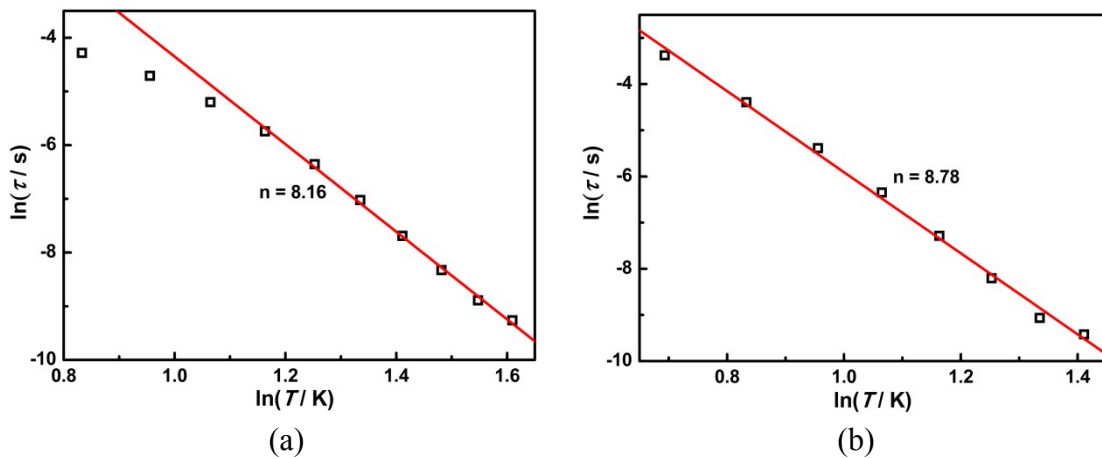


Fig. S12 $\ln\tau$ vs. $\ln T$ plots for complexes **1** (a) and **2** (b). The red lines are the best fits to a power law.

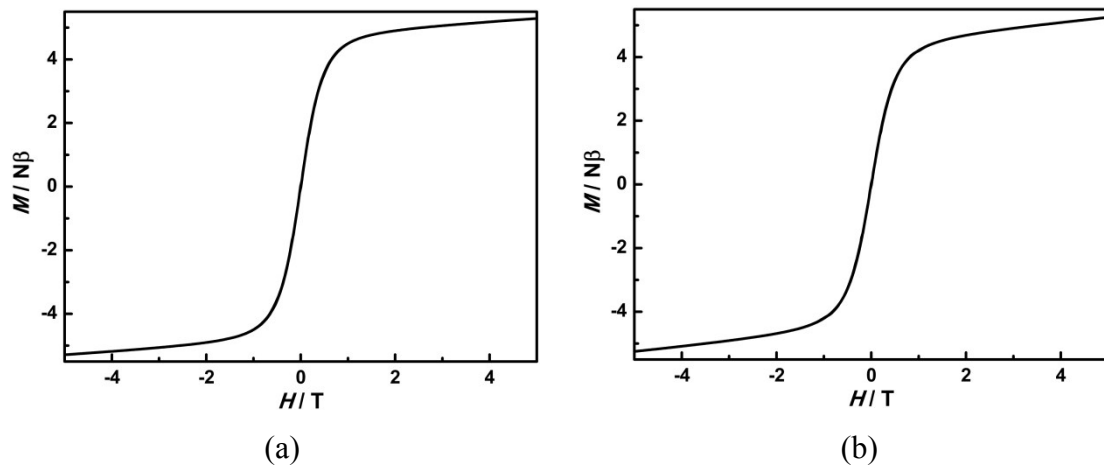


Fig. S13 Field dependence of the magnetization at 2K for complexes **1** (a) and **2** (b).

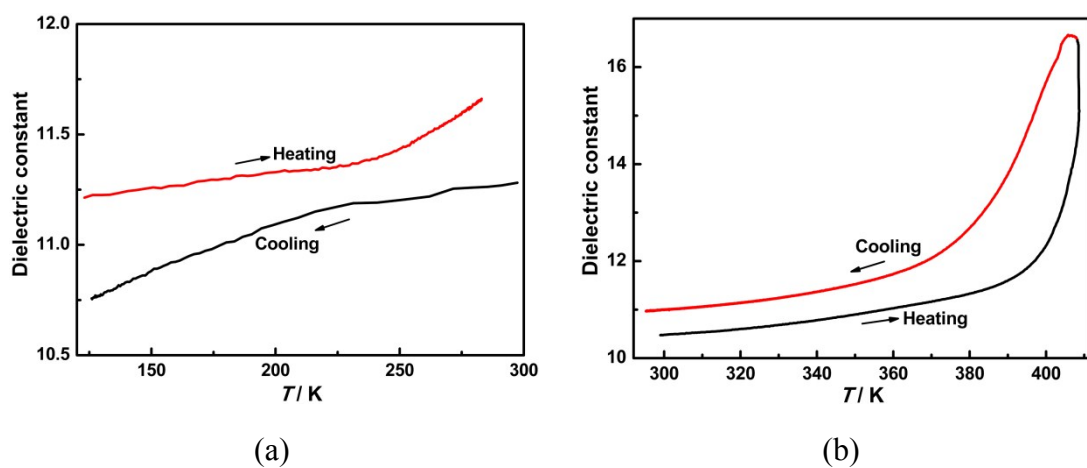


Fig. S14 Temperature dependence of the dielectric constant at 1MHz for complex **2**.

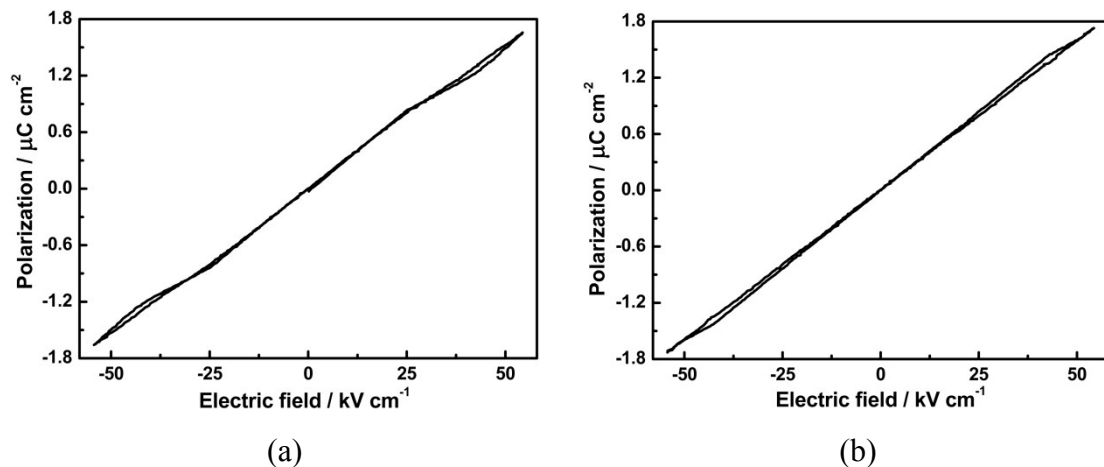


Fig. S15 Selective P-E curves for complex **2** at 253K (a) and 273K (b).